

# HybridSplat: Fast Reflection-baked Gaussian Tracing using Hybrid Splatting

Chang Liu Beijing Normal University	Hongliang Yuan Xiaomi Inc.	Lianghao Zhang Xiaomi Inc.
Sichao Wang Beijing Normal University	Jianwei Guo Beijing Normal University	Shi-Sheng Huang Beijing Normal University

## Abstract

Rendering complex reflection of real-world scenes using 3D Gaussian splatting has been a quite promising solution for photorealistic novel view synthesis, but still faces bottlenecks especially in rendering speed and memory storage. This paper proposes a new **Hybrid Splatting** (HybridSplat) mechanism for Gaussian primitives. Our key idea is a new reflection-baked Gaussian tracing, which bakes the view-dependent reflection within each Gaussian primitive while rendering the reflection using tile-based Gaussian splatting. Then we integrate the reflective Gaussian primitives with base Gaussian primitives using a unified hybrid splatting framework for high-fidelity scene reconstruction. Moreover, we further introduce a pipeline-level acceleration for the hybrid splatting, and reflection-sensitive Gaussian pruning to reduce the model size, thus achieving much faster rendering speed and lower memory storage while preserving the reflection rendering quality. By extensive evaluation, our HybridSplat accelerates about 7 $\times$  rendering speed across complex reflective scenes from Ref-NeRF, NeRF-Casting with 4 $\times$  fewer Gaussian primitives than similar ray-tracing based Gaussian splatting baselines, serving as a new state-of-the-art method especially for complex reflective scenes. Please visit our website for more details and information: <https://aetheryne.github.io/HybridSplat/>

## 1. Introduction

3D Gaussian Splatting (3DGS) [29] has achieved remarkable success for complex scene rendering, which enables various applications such as photorealistic novel view synthesis [24, 34, 39, 48], scene relighting [4, 15, 35, 62], and scene editing [7, 8, 56]. However, it still remains challenging for 3DGS to model complex reflections of real-world scenes, which is mainly due to the limited expressiveness of the Spherical Harmonics (SH) [55].

To accurately capture the reflective lighting effects of real-world scenes, some works (such as Gaussian-Shader [28], 3DGS-DR [30], GS-IR [36], GS-ID [9]) adopt

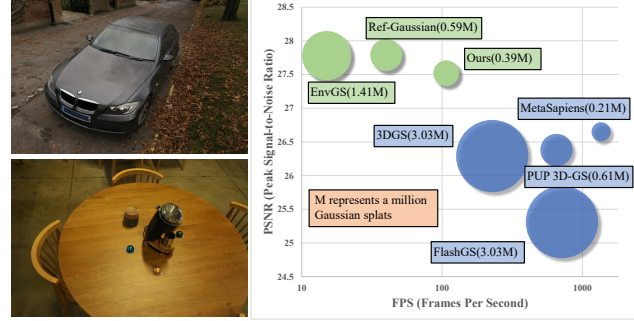


Figure 1. The novel view rendering results of our HybridSplat (left) and performance comparison with different 3D Gaussian splatting approaches (right). As ray-tracing based 3DGS (marked green), our HybridSplat outperforms latest baselines such as EnvGS [55], Ref-Gaussian [58] with much faster rendering speed and fewer Gaussian primitives, while preserving similar rendering quality which is consistently better than other non-ray-tracing based 3DGS approaches (marked blue). The circle size represents the corresponding Gaussian primitive numbers.

to additionally model the environmental lighting and perform joint optimization of 3DGS and lighting for accurate 3DGS reconstruction, but are limited to model high-frequency reflection details. Inspired by the impressive Gaussian ray-tracing [42] to model secondary lighting effects, recent works such as IRGS [17], EnvGS [55] proposed to use 2D Gaussian ray-tracing with accurate ray-splat intersection for expressive view-dependent reflection, which achieve remarkable reflection reconstruction quality even under near-field scenarios. Although the expressive success has been achieved in high-fidelity rendering quality, one major bottleneck of these works is that the Gaussian ray-tracing is performed in a pixel-wise manner. Despite real-time rendering can be achieved using the hardware acceleration (NVIDIA OptiX [45]) with geometry proxies like BVH (3DGRT [42], 3DGUT) [54], mesh (MeshSplat [49]) or without [6, 16], the rendering speed is still limited due to the huge computation for Gaussian ray-tracing. Moreover, extensive memory storage is also essentially needed due to massive redundant Gaussian primitives [11].



Figure 2. The visual comparison results between our **HybridSplat** and similar ray-tracing based Gaussian splatting like EnvGS [55] along with the 3DGS. The rendering speed (FPS), quality (PSNR) and Gaussian primitive number (GS) are also demonstrated respectively, where 'M' is short for million.

On the other hand, recent works such as SpeedySplat [18], MetaSapiens [38], FlashGS [13] propose to accelerate the computing pipeline of the 3D Gaussian splatting, which achieve remarkable rendering speed acceleration. Gaussian primitive pruning (PUP-3D [19]) or vector quantization based compression[11, 33] further reduce the 3D Gaussian primitive storage. However, most of these pioneering works focus on original 3DGS's splatting pipeline but not Gaussian ray-tracing. Although recent works like [5] provide hardware-accelerated Gaussian ray-tracing at test time, it still remains under-explored to significantly accelerate the Gaussian ray-tracing's rendering speed while massively reducing the Gaussian redundancy, for high fidelity complex reflection rendering (both training and testing) in very fast rendering speed and low memory storage.

To address the above issues, this paper introduces a new and novel hybrid Splatting (HybridSplat) mechanism to reconstruct real-world scene with complex reflection, but in much faster rendering speed and lower memory storage. The key point of our HybridSplat is a novel **Reflection-baked Gaussian Tracing** over 2D Gaussian primitives, which bakes the reflection within each Gaussian primitive and renders the reflection image via more efficient tile-based Gaussian splatting, thus avoiding the time-consuming pixel-wise Gaussian ray-tracing[6, 16, 42, 54]. To preserve high-frequency reflection rendering[17, 55], we integrate reflective Gaussian primitives with base Gaussian primitives to model the view-dependent appearance using a unified **Hybrid Splatting**, where the reflective attribution is adaptively blended with the base attribution. Moreover, we further propose unified splatting pipeline acceleration to improve the rendering speed, and adopt reflection-sensitive Gaussian pruning to adaptively prune redundant Gaussian primitives. In this way, we accurately reconstruct the complex reflections of real-world scenes, and achieve

much faster rendering speed and lower memory storage simultaneously as shown in Fig. 1.

To evaluate the effectiveness of our HybridSplat, we conduct extensive experiments on public benchmarks such as Ref-NeRF [50], NeRF-Casting [51], Mip-NeRF 360 [3], Tasks & Temples [32] and Deepblending [20] datasets, by comparing with similar ray-tracing Gaussian splatting method like EnvGS[55], and other non-ray-tracing Gaussian splatting such as Speedy-Splat[18], MetaSapiens[38], FlashGS[13], PUP 3D-GS[19] aimed at 3DGS acceleration. Specifically, on average our HybridSplat achieves about  $7\times$  faster rendering speed and  $4\times$  fewer Gaussian primitives than EnvGS[55], while preserving similar complex reflection rendering quality like EnvGS[55], much better than those non-ray-tracing alternatives as shown in Fig. 2. Besides, although Ref-Gaussian [58] focus on objects but not complex scenes like our scenario, our HybridSplat also achieves nearly  $2\times$  faster rendering speed and  $2\times$  fewer Gaussian primitives, with better rendering quality for complex reflective scenes.

## 2. Related Work

**3D Scene Reconstruction.** Reconstructing 3D scenes using deep implicit function [25, 26, 52, 63] or neural radiance fields (NeRF) [41] has motivated 3D novel view synthesis applications [22, 27, 37]. However, the dense volumetric rendering that NeRF required leads to slow rendering speeds which limit the practical use, despite subsequent efforts made to accelerate the rendering speed using explicit data structure [2, 14, 43], re-parameterizations [1] and rendering caching [21, 47]. 3DGS [29] and 2DGGS[23] overcome such drawbacks with anisotropic Gaussian primitives using efficient tile-based splatting to significantly improve the rendering speed, inspiring many photo-realistic novel

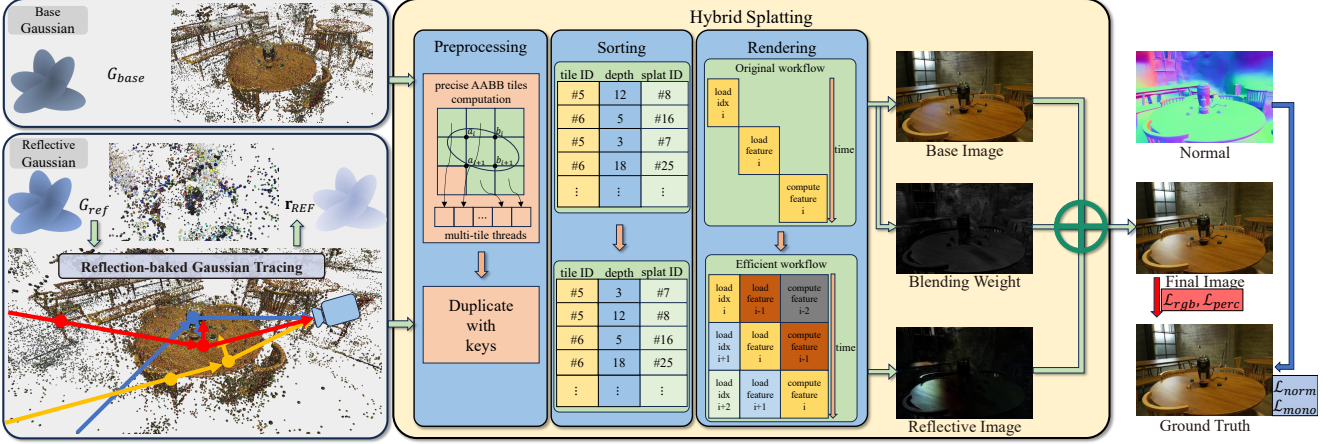


Figure 3. **Pipeline of HybridSplat.** We first reconstruct complex reflective scenes with base Gaussians  $G_{base}$  and reflective Gaussians  $G_{ref}$ , where the latter bake the reflection using a novel reflection-baked Gaussian tracing (left). Then these Gaussians are efficiently rendered using our hybrid splatting (middle), with specific pipeline acceleration at the preprocessing (more precise AABB-tiles) and rendering (more efficient execution flow) stages, for the final image rendering (right).

view synthesis [34, 39, 48] and scene manipulation such as relighting [4, 15, 35, 62] and editing [7, 8, 56]. However, their rendering quality of complex reflection effects are still limited often with artifacts like blurriness or ghost.

To model complex reflections of real-world scenes, some works introduced additional environment maps (Gaussian shader[28], 3DGS-DR[30]) or neural light field (GS-IR [36], GS-ID [9]) to model the lighting for improved reflection rendering ability, but still limited to capture distant lighting without enough high-frequency reflection details. Ray-tracing based Gaussian splatting [16, 42, 54] proposed to model the secondary lighting effects by tracing the Gaussian primitives. Recent works such as IRGS [17], EnvGS[55] choose to perform 2DGS-based ray-tracing with more accurate ray-splat intersection, thus obtaining better reflection reconstruction. Ref-Gaussian [58] and subsequent work [61] adopt to trace the shading and perform physically-based rendering with BRDF materials splatting for highly accurate reflective objects rendering. However, due to the requirement of pixel-wise ray-tracing, these works suffer from limited rendering speed, and face challenges for much faster reflective scene rendering.

Our work is inspired by the recent ray-tracing based Gaussian splatting works, but proposes a more efficient per-Gaussian ray-tracing, and more importantly, introduces effective splatting pipeline level acceleration with reflection-sensitive Gaussian pruning, while preserving the reflection rendering quality from real-world scene reconstruction but not only objects [58, 61].

**Gaussian Splatting Acceleration.** In order to improve the rendering speed of 3DGS, some works focus on pruning redundant Gaussian primitives according to significance score for each Gaussian respectively. Lightgaussian[10],

Mini-Splatting[12] and RadSplat[44] compute the integrated contribution of each Gaussian across all input images. MetaSapiens[38] proposes an efficient-aware pruning technique, along with Foveated Rendering (FR) method, utilizing the characteristic that humans' visual system are not acute enough in peripheral regions. PUP 3D-GS[19] proposes a principled spatial sensitivity pruning score, calculated as second-order approximation of the reconstruction error with respect to the spatial parameters of each Gaussian. Based on it, Speedy-Splat[18] replaces the parameters with those of projected 2D Gaussians, lowering the memory requirements, meanwhile improving calculating speeds. The Gaussian models can be further compressed using the quantization based compression techniques[11, 33].

Besides, some works like Mini-Splatting[12] introduces blur split and depth reinitialization strategies in densification to reorganize the spatial distribution of Gaussians, thereby limiting the number of Gaussians, thus improving rendering speed. Taming 3DGS[40] controls the model size to an exact predefined budget. FlashGS[13] introduces an efficient and precise intersection algorithm and pipeline optimizations. However, most of these Gaussian splatting methods focus on the original splatting but not ray-tracing based Gaussian splatting. In contrast, our work proposed to accelerate the Ray-tracing Gaussian splatting via unified hybrid splatting, which achieves much faster rendering speed and lower memory storage.

### 3. Method

Given a set of input images  $\mathcal{I} = \{I_i | i = 1, \dots, N\}$  captured from a complex reflective 3D scene with known camera poses  $\mathcal{T}$ , our goal is to reconstruct the 3D scene with a set of *base Gaussian* primitives  $G_{base} = \{g_b^i | i = 1, \dots, M_b\}$  and

reflective Gaussian primitives  $G_{ref} = \{g_r^i | i = 1, \dots, M_r\}$ , which can perform image rendering  $\mathbf{c}$  at any novel view  $\mathcal{T}_v$  with a hybrid splatting over  $G_{base}$  and  $G_{ref}$ , i.e.,  $\mathbf{c} = HybridSplat(G_{base}, G_{ref}, \mathcal{T}_v)$ .

### 3.1. Hybrid Splatting

Our hybrid splatting (HybridSplat) follows similar tile-based Gaussian rasterization as original 3DGS[29], which consists of three main stages including preprocessing, sorting and rendering as shown in Fig. 3. The key difference is that our HybridSplat has two sub-branches, each of which splats the base Gaussian primitives  $G_{base}$  (for base image rendering  $\mathbf{c}_{base}$ ) and reflective Gaussian primitives  $G_{ref}$  (for reflective image  $\mathbf{c}_{ref}$ ) respectively, and blends the final image rendering  $\mathbf{c}$  using a blending weight  $\beta$  as:

$$\mathbf{c} = (1 - \beta) \cdot \mathbf{c}_{base} + \beta \cdot \mathbf{c}_{ref}. \quad (1)$$

We adopt 2DGS[23] primitives as the basic representations of both  $G_{base}$  and  $G_{ref}$ , due to its benefit in compact geometry structure and accurate ray-splat intersection. One important difference between a base Gaussian  $g_b^i$  and reflective Gaussian  $g_r^i$ , is that  $g_b^i$  restores SH attribution (to calculate the view-dependent color  $\mathbf{c}_{SH}^i$ ) while  $g_r^i$  doesn't restore SH but reflection coefficients  $\mathbf{r}^i$  (to blend the baked reflection  $\mathbf{r}_{REF}^i$ ) instead, with other attributions remaining the same. Thus we splat  $\mathbf{c}_{base}$  and  $\mathbf{c}_{ref}$  as:

$$\mathbf{c}_{base} = \sum_j^{M_b} T_j \alpha_j \mathbf{c}_{SH}^j, \quad \mathbf{c}_{ref} = \sum_j^{M_r} T_j \alpha_j \mathbf{r}_{REF}^j, \quad (2)$$

with  $T_j = \Pi_{k=1}^{j-1} (1 - \alpha_k)$ ,  $M_b$  and  $M_r$  are the Gaussian numbers of  $G_{base}$  and  $G_{ref}$  respectively. Moreover, we bake each  $g_r^i$ 's reflection  $\mathbf{r}_{REF}^i$  via a new reflection-baked Gaussian tracing (Sec. 3.2), to model the high-frequency details of environmental reflections. In this way, we formulate both the base Gaussian splatting and reflective Gaussian tracing into a unified splatting pipeline, which can benefit the subsequent splatting acceleration (Sec. 3.3) and reflection-sensitive Gaussian pruning (Sec. 3.4) for fast rendering with less redundant Gaussian primitives, while preserving the high quality rendering simultaneously.

### 3.2. Reflection-baked Gaussian Tracing

Unlike current pixel-wise Gaussian ray-tracing[17, 42, 54, 55], we perform a reflection-baked Gaussian tracing at per-Gaussian level, and blend the traced Gaussians' reflective coefficients  $\{\mathbf{r}^k\}$  as baked reflection attributes  $\mathbf{r}_{REF}$ . In this way, the ray number to be traced is modified from pixels' size to reflective Gaussians' size. Once the reflective Gaussians' size is effectively pruned via our thereafter reflection-sensitive Gaussian pruning (Sec.3.4), the traced rays can be reduced in massive amount, thus providing much faster Gaussian ray-tracing.

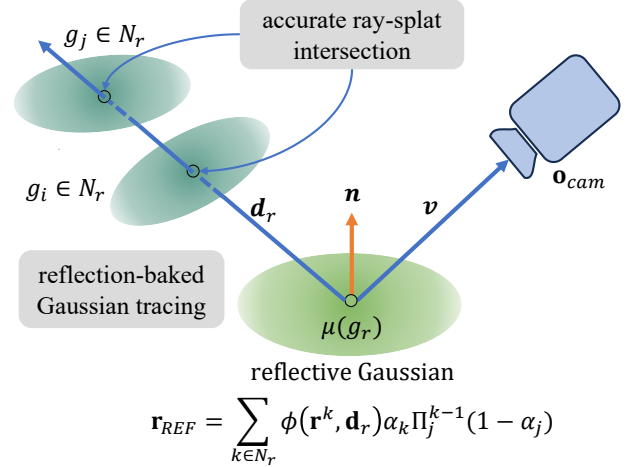


Figure 4. **Reflection-baked Gaussian Tracing.** This process bakes the reflection within each reflective Gaussian primitive, allowing for unified splatting with base Gaussian.

Specifically, as shown in Fig. 4, for a reflective Gaussian  $g_r$  at any novel view  $\mathcal{T}_v$ , we calculate its' splatting direction  $v$  as  $v = \mu(g_r) - \mathbf{o}_{cam}$ , where  $\mu(g_r)$  is the centroid position of  $g_r$  and  $\mathbf{o}_{cam}$  is the center position of camera view. Then we trace the reflective ray  $\mathbf{d}_r$  starting from  $g_r$ 's centroid position  $\mu(g_r)$  as

$$\mathbf{d}_r = v - 2(v \cdot n)n,$$

with  $n$  is  $g_r$ 's normal attribute. Thereafter, we blend the traced reflective Gaussians' reflection coefficients to get the baked reflection  $\mathbf{r}_{REF}$  as:

$$\mathbf{r}_{REF} = \sum_{k \in N_r} \phi(\mathbf{r}^k, \mathbf{d}_r) \alpha_k \Pi_j^{k-1} (1 - \alpha_j), \quad (3)$$

where  $N_r$  is the index set of traced reflective Gaussians,  $\phi(\mathbf{r}^k, \mathbf{d}_r)$  is the weighted function for ray  $\mathbf{d}_r$  intersecting with reflective Gaussian  $g_k$ , please refer to our supplementary materials for more details.

### 3.3. Hybrid Splatting Pipeline Acceleration

Since both the base Gaussians and reflective Gaussians are splatted using unified hybrid splatting, we further propose to accelerate the computing pipeline of our hybrid splatting, using more compact AABB-tiles calculation in the preprocessing stage and an efficient execution workflow in the rendering stage respectively.

Unlike previous tile estimation methods [13, 18] which need explicit representations of 2D ellipse for fast redundant tile elimination, our base Gaussian and reflective Gaussian don't have such precisely explicit 2D ellipse since they are based on 2D Gaussian primitives. Thus, it is non-trivial to directly applying those strategies to our case. Instead, we

augment the 2D Gaussian primitives to thin 3D Gaussian primitives, by enlarging rotation vectors  $\mathbf{R} = [\mathbf{t}_u, \mathbf{t}_v] \rightarrow [\mathbf{t}_u, \mathbf{t}_v, \mathbf{t}_u \times \mathbf{t}_v]$  and scaling vectors  $\mathbf{S} = (\mathbf{s}_u, \mathbf{s}_v) \rightarrow (\mathbf{s}_u, \mathbf{s}_v, \epsilon)$  where  $\epsilon$  is a small constant value. In this way, we can approximate the explicit 2D ellipse of both base Gaussians and reflective Gaussians. Thereafter, as shown in Fig. 3, for each Gaussian primitive’s projection, we explicitly calculate the precise AABB box, and further determine whether the  $i$ -th tile  $[\mathbf{a}_i, \mathbf{b}_i, \mathbf{a}_{i+1}, \mathbf{b}_{i+1}]$  intersects the 2D ellipse or not, using a multi-tile threading parallelized fast tile-ellipse intersection. Please refer to our supplementary materials for more details of fast tile-ellipse intersection.

As for the rendering stage of the original 3DGS pipeline, each tile need first fetch index from the global memory and then calculate transmittance and color within GPU in a one-by-one manner, which has very high time cost. Instead, we propose to use a more efficient parallelized fetching and calculating way. Specifically, as shown in Fig. 3, we first load as many data indices and attributes to the global memory as possible. Then we fetch the  $step_i$ ’s index from the global memory, retrieve the  $step_{i-1}$ ’s feature attributes, and calculate the  $step_{i-2}$ ’s rendering computation. Thus, our execution workflow is not serial, *i.e.*, fetching  $step_i$ ’s index  $\rightarrow$  retrieving  $step_i$ ’s feature attributes  $\rightarrow$  calculating  $step_i$ ’s rendering parameters, but in a much faster parallelized fetching-and-calculating manner.

### 3.4. Reflection-Sensitive Gaussian Pruning

Finally, we perform Gaussian pruning [19] for both base Gaussians  $G_{base}$  and reflective Gaussians  $G_{ref}$  jointly based on our hybrid splatting. One important difference in our Gaussian pruning is that we can perform reflection-sensitive Gaussian pruning, since our final image rendering requires the reflection sensitive weight  $\beta$ . Thus, our Gaussian pruning can preserve better reflection adaptively than strategies naively applying previous Gaussian pruning [18, 19].

Specifically, we adopt similar pruning score  $\tilde{U}_i$  for each Gaussian primitive  $g_i$  ( $g_i \in \{G_{base}, G_{ref}\}$ ) like [19] as:

$$\tilde{U}_i = (\nabla_{g_i} I_G(G_{base}, G_{ref}))^2. \quad (4)$$

Then we set the blending weight  $\beta$  fixed, thus reformulating the pruning score as:

$$\tilde{U}_i = (1 - \beta) \cdot (\nabla_{g_b^i} \frac{\partial I_G}{\partial G_{base}})^2 + \beta \cdot (\nabla_{g_r^i} \frac{\partial I_G}{\partial G_{ref}})^2, \quad (5)$$

where  $\nabla_{g_b^i}$ ,  $\frac{\partial I_G}{\partial G_{base}}$ ,  $\nabla_{g_r^i}$  and  $\frac{\partial I_G}{\partial G_{ref}}$  can be efficiently obtained by the back-propagation of our hybrid splatting. In this way, we can effectively reduce the redundant Gaussian primitives for both base Gaussians and reflective Gaussians in a unified manner, while preserving the reflection sensitivity as much as possible. We evaluate the effectiveness of our reflection-sensitive Gaussian pruning as shown in Sec. 4.5.

## 4. Experiments

### 4.1. Implementation Details

We implement our model with PyTorch[46] following Easyvolcap[57] framework and using Adam optimizer[31] to train. We first train the base Gaussians and reflective Gaussians using multiple-view images as inputs, and reconstruct the real-world scenes. Then we further conduct reflection-sensitive Gaussian pruning to reduce the redundant Gaussian primitives. In the training stage, we perform base Gaussian warm-up training within 6 epochs, and it takes on average 120 epochs to obtain the final convergence. As for the pruning stage, the pruning ratio are set as 0.05 at every 500 iterations. All of the models’ training, pruning and comparing experiments are implemented on a single NVIDIA RTX 4090 GPU platform.

**Training Losses.** During the hybrid splatting training, we adopt similar training losses to EnvGS [55], which consist of RGB reconstruction loss  $\mathcal{L}_{rgb}$ , normal consistency regularization  $\mathcal{L}_{norm}$ , monocular normal supervision loss  $\mathcal{L}_{mono}$  and perceptual loss  $\mathcal{L}_{perc}$ . Please refer to our supplementary materials for more details.

### 4.2. Datasets, Metrics and Baselines

To evaluate our HybridSplat, we first conduct evaluations on datasets with complicated specular reflections, including real-world Ref-NeRF[50] dataset and NeRF-Casting dataset[51]. Besides, we also test our models on datasets which are commonly used in prior works, including Mip-NeRF 360 dataset[3], Tanks & Temples[32] and Deep-Blending Datasets[20], to show the generalization ability of our HybridSplat. We follow the training and testing splits mentioned in prior works[29, 55], which maintain the same across all datasets and methods. For metrics, we use PSNR, SSIM[53] and LPIPS[60] to evaluate the image rendering quality during the novel view synthesis application.

We mainly compare our HybridSplat with similar ray-tracing Gaussian splatting like EnvGS[55], and also previous non-ray-tracing alternatives aimed at improving rendering speeds on original 3DGS[29], including Speedy-Splat[18], MetaSapiens[38], FlashGS[13] and PUP 3DGS[19], all the works mentioned above don’t take ray tracing into account. Besides, we also compare with Ref-Gaussian [58], though they focus on objects while ours on complex scenes.

### 4.3. Quantitative Evaluation

We first evaluate our method on three real-world scenes from the Ref-NeRF dataset[50] and four other scenes from NeRF-Casting dataset[51], which feature complex specular reflection appearance, the quantitative results are shown in Tab. 1. As the results show, our method achieves high-quality rendering with competitive quality in ray-tracing

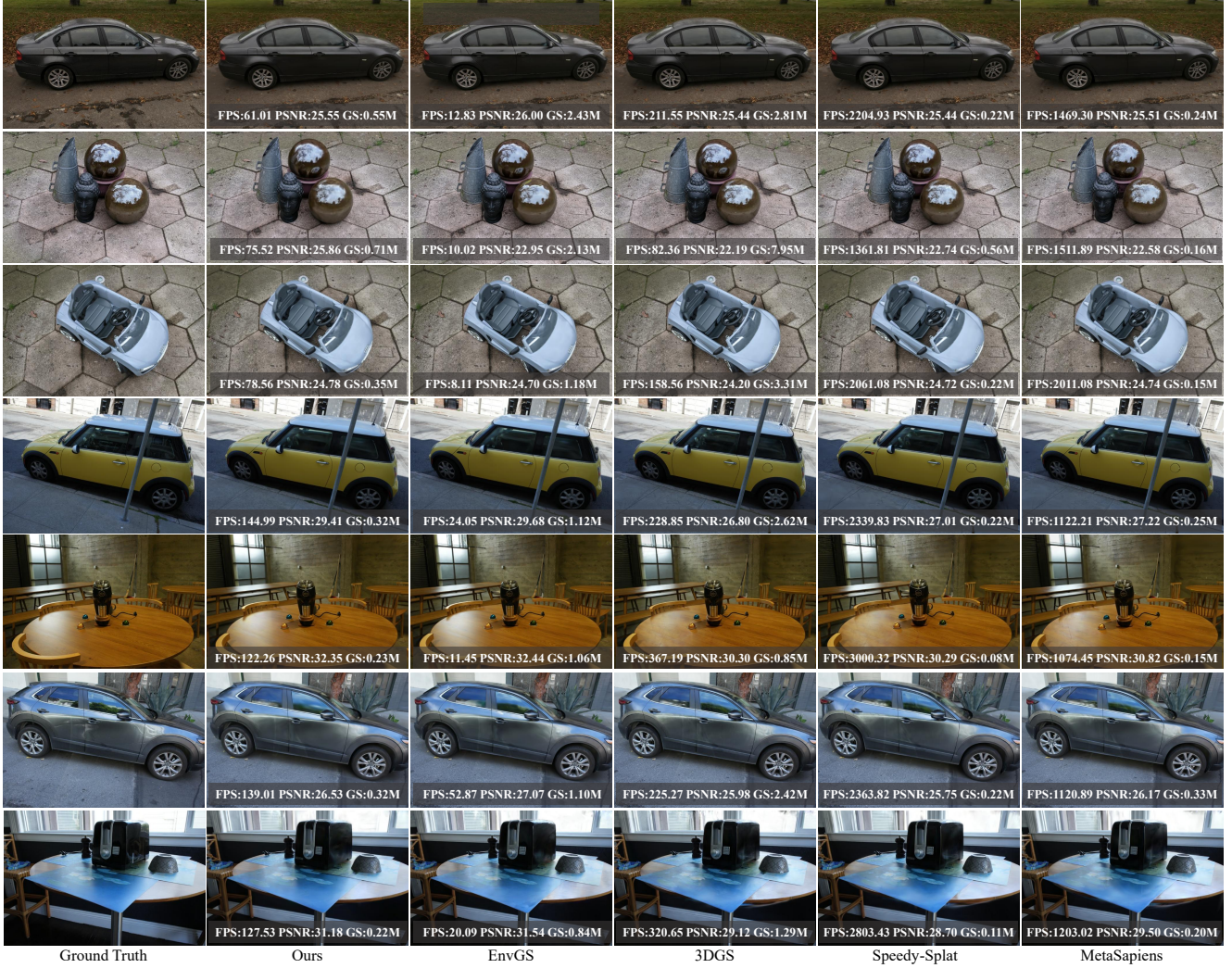


Figure 5. **Qualitative comparison on Ref-NeRF[50] and NeRF-Casting[51] dataset.** Our method achieves much faster rendering speed and few Gaussian primitives than EnvGS[55], with high image quality, better than other 3DGS baselines.

Methods	Ref-NeRF Real Scenes [50]			NeRF-Casting Shiny Scenes [51]				speedup	GS number $\downarrow$
	PSNR $\uparrow$	SSIM $\uparrow$	LPIPS $\downarrow$	PSNR $\uparrow$	SSIM $\uparrow$	LPIPS $\downarrow$	FPS $\uparrow$		
3DGS[29]	23.94	0.641	<b>0.265</b>	28.05	0.847	0.191	227.78	1x	3033253
Speedy-Splat[18]	<b>24.30</b>	<b>0.658</b>	0.324	27.94	0.832	0.238	<b>2305.03</b>	<b>10.12x</b>	234714
MetaSapiens[38]	24.28	0.629	0.330	<b>28.43</b>	0.845	0.205	1358.98	5.97x	<b>212662</b>
FlashGS[13]	22.93	0.535	0.317	27.10	0.818	0.240	714.97	3.14x	3033253
PUP 3D-GS[19]	23.78	0.644	0.289	28.33	<b>0.858</b>	<b>0.180</b>	653.56	2.87x	606650
EnvGS[55]	24.55	0.666	0.282	<b>30.21</b>	0.872	<b>0.158</b>	15.05	1x	1408937
Ref-Gaussian[59]	<b>24.61</b>	<b>0.685</b>	<b>0.252</b>	30.17	<b>0.873</b>	0.161	65.77	4.37x	592099
Ours	24.40	0.664	0.280	29.87	0.864	0.175	<b>106.98</b>	<b>7.11x</b>	<b>385722</b>

Table 1. **Quantitative comparison on Ref-NeRF and NeRF-Casting Shiny Scenes datasets.** Our method realizes high-quality rendering, while renders the fastest among tracing methods.

based Gaussian splatting, while rendering much faster than EnvGS [55] and Ref-Gaussian [58] with fewer Gaussian

primitives. Specifically, in the quality aspect, our method are competitive in all the metrics with other tracing meth-

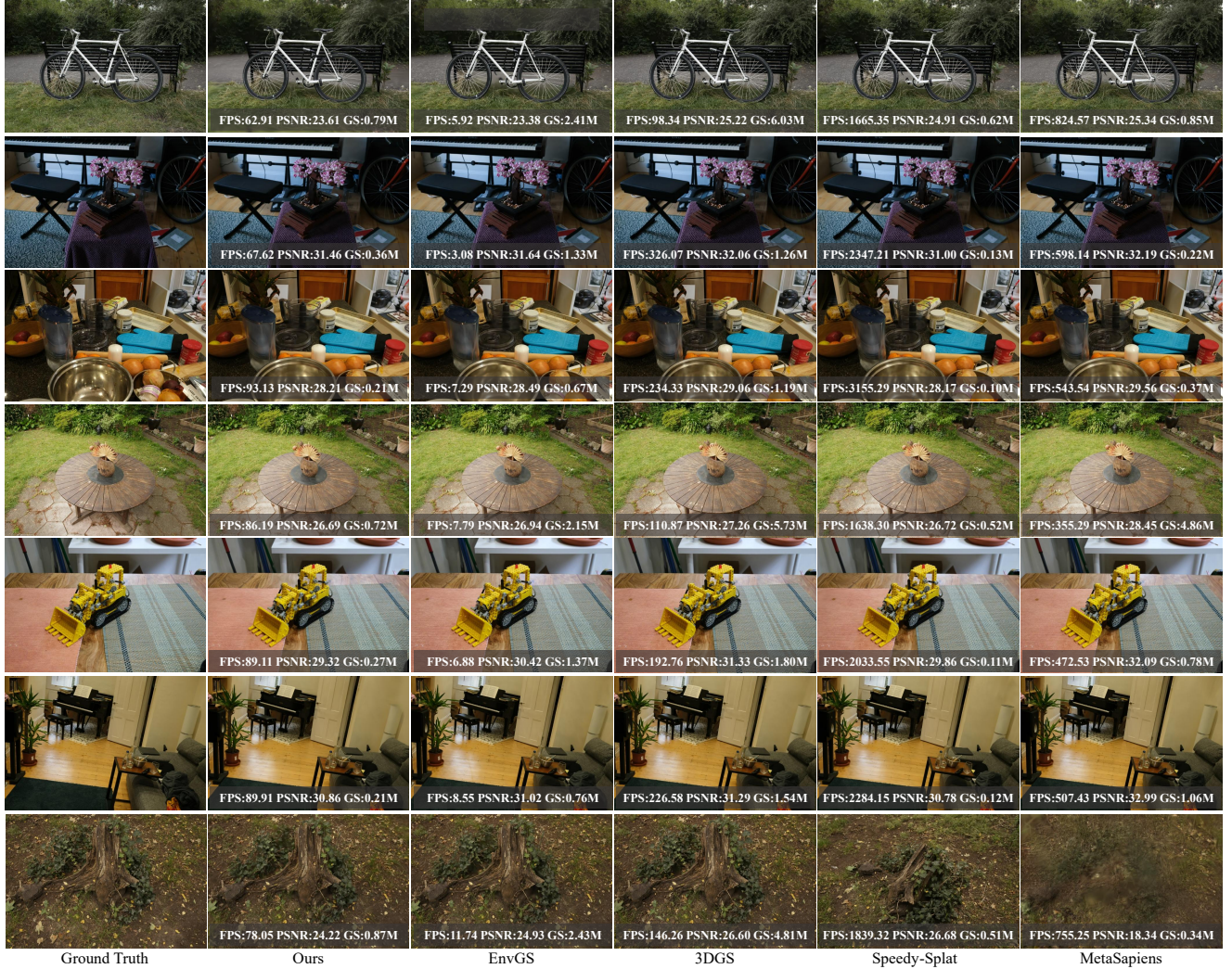


Figure 6. **Qualitative comparison on Mip-NeRF 360 dataset.** Similarly, our method achieves much faster rendering speed and few Gaussian primitives than EnvGS[55], with high image quality, better than other 3DGS baselines.

ods, and renders the fastest among them with an average of  $7\times$  faster than EnvGS and nearly  $2\times$  than Ref-Gaussian, while using fewer Gaussian primitives with average  $4\times$  fewer than EnvGS and  $2\times$  fewer than Ref-Gaussian respectively. Although our HybridSplat does not achieve similar-level rendering speed than those pipeline acceleration approaches, we can achieve consistently better rendering quality especially for complex reflective scenes. This conclusion also holds for other complex scene datasets of Mip-NeRF 360 dataset[3], Tanks & Temples[32] and Deep-Blending Datasets[20], please refer to our supplementary materials for the detail quantitative comparison.

#### 4.4. Qualitative Evaluation

We also conduct per-scene breakdown qualitative evaluations on Ref-NeRF[50] and NeRF-Casting[51] datasets as shown in Fig. 5. As for details of the rendered image qual-

ity, the reflection on the screenshield of *toycar* scene(3rd row from the top), the large reflection light area on the left part of the table in the *grinder* scene(5th row from the top) in Fig. 5 and the reflected light on the cardboard of *toaster* scene(7th row from the top) are all obvious indications for the superiority of our method in rendered image quality, showing that reflection-baked Gaussian tracing can represent highlights well. We also provide qualitative comparisons on Mip-NeRF 360 dataset[3], Tanks & Temples[32] and DeepBlending Datasets[20], the qualitative results on Mip-NeRF 360 dataset are shown in Fig. 6. Since these scenes do not contain complex reflection appearance, both EnvGS and HybridSplat do not show much quality superior, but HybridSplat still the fastest among ray-tracing methods. For more results on Tanks & Temples[32] and DeepBlending[20], please refer to our supplementary materials.



Figure 7. Qualitative comparison on **hatchback** scene of NeRF-Casting dataset. Compared with EnvGS baseline, our reflection-based Gaussian tracing, reflection-sensitive pruning and pipeline acceleration strategies takes effects for much faster rendering speed respectively.

Methods	base GS↓	ref. GS↓	PSNR↑	FPS↑
+RB-Tracing	1605565	551857	25.47	2.25
Naive Pruning	<b>474207</b>	70887	25.47	27.82
Our Pruning	489347	<b>55752</b>	<b>25.49</b>	<b>36.92</b>

Table 2. Quantitative Comparison of our pruning with naive on *sedan* scene of Ref-NeRF[50] dataset.

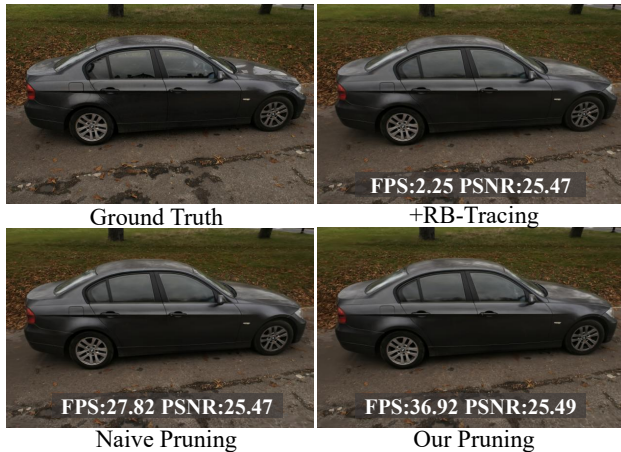


Figure 8. Qualitative comparison of our pruning with naive on *sedan* scene of Ref-NeRF[50] dataset.

Methods	PSNR↑	SSIM↑	LPIPS↓	FPS↑
EnvGS	<b>30.21</b>	<b>0.872</b>	<b>0.158</b>	18.60
+RB-Tracing	30.06	0.871	0.163	41.44
+Pruning	30.00	0.867	0.174	67.52
+P-Acc	29.87	0.864	0.175	<b>106.98</b>

Table 3. Ablation Studies on NeRF-Casting[51] dataset.

#### 4.5. Ablation Studies

We conduct ablation studies on key components of our method, including reflection-baked Gaussian tracing, reflection-sensitive Gaussian pruning and Hybrid Splatting pipeline acceleration. Here we choose EnvGS as baseline to conduct the ablation studies. The quantitative and qualitative results are shown in Tab. 3 and Fig. 7 respectively.

**Reflection-baked Gaussian Tracing.** We first replace the ray-tracing module of EnvGS[55] with our reflection-

baked Gaussian tracing ('+RB-Tracing'). Then we perform our pruning strategy ('+Pruning'), leading to much fewer Gaussian primitives and faster rendering speed. This also makes it possible to implement our unified pipeline acceleration ('+P-Acc'), improving rasterization speed greatly, which is also a key component of our work. The "+RB-Tracing" in Tab. 3 shows that our reflection-baked tracing significantly improves rendering speed.

**Reflection-sensitive Gaussian Pruning.** Inspired by Speedy-Splat[18], a large portion of Gaussian splats are redundant. Instead of implementing pruning in the process of densification, we implement pruning after densification to show the pruning effects more evidently. This pruning process significantly reduces the Gaussian number, improving the rendering speed without obviously affecting image quality, as shown in Tab. 1. The "+Pruning" line in Tab. 3 shows that our pruning preserves image quality, while improving rendering speed. To show the necessity of our pruning strategy, we compare our pruning with naive pruning from Speedy-Splat[18] ('Naive Pruning'), which calculates base Gaussian and reflective Gaussian pruning scores differently without considering reflection-sensitive weights. The qualitative and quantitative results are shown in Fig. 8 and Tab. 2 respectively, without our reflection-sensitive weights, the pruning process tends to prune in favor of base Gaussians, leaving more reflective Gaussians, which participate in more time-consuming ray tracing process.

## 5. Conclusion

In this paper, we introduce HybridSplat with a novel reflection-baked Gaussian splatting, which benefits high rendering speed and less memory storage using hybrid splatting with unified pipeline acceleration and reflection-sensitive Gaussian pruning. One main drawbacks of our reflection-baked Gaussian tracing comes from the very near-field reflections in single object scenario, and also more precise Gaussian normal estimation are still needed as like other ray-tracing Gaussian splatting methods [10, 55], which we leave for future works. We hope our HybridSplat could inspired subsequent works for more efficient ray-tracing based Gaussian splatting in both training and testing, while preserving the rendering quality especially for complex reflective scenes.

## References

[1] Jonathan T Barron, Ben Mildenhall, Matthew Tancik, Peter Hedman, Ricardo Martin-Brualla, and Pratul P Srinivasan. Mip-nerf: A multiscale representation for anti-aliasing neural radiance fields. In *Proceedings of the IEEE/CVF international conference on computer vision*, pages 5855–5864, 2021. 2

[2] Jonathan T Barron, Ben Mildenhall, Dor Verbin, Pratul P Srinivasan, and Peter Hedman. Mip-nerf 360: Unbounded anti-aliased neural radiance fields. In *Proceedings of the IEEE/CVF conference on computer vision and pattern recognition*, pages 5470–5479, 2022. 2

[3] Jonathan T. Barron, Ben Mildenhall, Dor Verbin, Pratul P. Srinivasan, and Peter Hedman. Mip-nerf 360: Unbounded anti-aliased neural radiance fields. In *2022 IEEE/CVF Conference on Computer Vision and Pattern Recognition (CVPR)*, pages 5460–5469, 2022. 2, 5, 7

[4] Zoubin Bi, Yixin Zeng, Chong Zeng, Fan Pei, Xiang Feng, Kun Zhou, and Hongzhi Wu. Gs3: Efficient relighting with triple gaussian splatting. In *SIGGRAPH Asia 2024 Conference Papers*, pages 1–12, 2024. 1, 3

[5] Samuel Rota Bulo, Nemanja Bartolovic, Lorenzo Porzi, and Peter Kortschieder. Hardware-rasterized ray-based gaussian splatting. In *Proceedings of the Computer Vision and Pattern Recognition Conference*, pages 485–494, 2025. 2

[6] Krzysztof Byrski, Marcin Mazur, Jacek Tabor, Tadeusz Dziarmaga, Marcin Kądziołka, Dawid Baran, and Przemysław Spurek. Raysplats: Ray tracing based gaussian splatting. *arXiv e-prints*, pages arXiv–2501, 2025. 1, 2

[7] Guo Chen, Jiarun Liu, Sicong Du, Chenming Wu, Deqi Li, Shi-Sheng Huang, Guofeng Zhang, and Sheng Yang. Gs-roadpatching: Inpainting gaussians via 3d searching and placing for driving scenes. *ACM SIGGRAPH Asia*, 2025. 1, 3

[8] Yiwen Chen, Zilong Chen, Chi Zhang, Feng Wang, Xiaofeng Yang, Yikai Wang, Zhongang Cai, Lei Yang, Huaping Liu, and Guosheng Lin. Gaussianeditor: Swift and controllable 3d editing with gaussian splatting. In *Proceedings of the IEEE/CVF conference on computer vision and pattern recognition*, pages 21476–21485, 2024. 1, 3

[9] Kang Du, Zhihao Liang, Yulin Shen, and Zeyu Wang. Gs-id: Illumination decomposition on gaussian splatting via adaptive light aggregation and diffusion-guided material priors. In *Proceedings of the IEEE/CVF International Conference on Computer Vision*, pages 26220–26229, 2025. 1, 3

[10] Zhiwen Fan, Kevin Wang, Kairun Wen, Zehao Zhu, Dejia Xu, and Zhangyang Wang. Lightgaussian: Unbounded 3d gaussian compression with 15x reduction and 200+ fps. In *Advances in Neural Information Processing Systems*, pages 140138–140158. Curran Associates, Inc., 2024. 3, 8

[11] Zhiwen Fan, Kevin Wang, Kairun Wen, Zehao Zhu, Dejia Xu, Zhangyang Wang, et al. Lightgaussian: Unbounded 3d gaussian compression with 15x reduction and 200+ fps. *Advances in neural information processing systems*, 37: 140138–140158, 2024. 1, 2, 3

[12] Guangchi Fang and Bing Wang. Mini-splatting: Representing scenes with a constrained number of gaussians. In *Computer Vision – ECCV 2024*, pages 165–181, Cham, 2024. Springer Nature Switzerland. 3

[13] Guofeng Feng, Siyan Chen, Rong Fu, Zimu Liao, Yi Wang, Tao Liu, Boni Hu, Lining Xu, Zhilin Pei, Hengjie Li, et al. Flashgs: Efficient 3d gaussian splatting for large-scale and high-resolution rendering. In *Proceedings of the Computer Vision and Pattern Recognition Conference*, pages 26652–26662, 2025. 2, 3, 4, 5, 6

[14] Sara Fridovich-Keil, Alex Yu, Matthew Tancik, Qinzhong Chen, Benjamin Recht, and Angjoo Kanazawa. Plenoxels: Radiance fields without neural networks. In *Proceedings of the IEEE/CVF conference on computer vision and pattern recognition*, pages 5501–5510, 2022. 2

[15] Jian Gao, Chun Gu, Youtian Lin, Zhihao Li, Hao Zhu, Xun Cao, Li Zhang, and Yao Yao. Relightable 3d gaussians: Realistic point cloud relighting with brdf decomposition and ray tracing. In *European Conference on Computer Vision*, pages 73–89. Springer, 2024. 1, 3

[16] Shrisudhan Govindarajan, Daniel Rebain, Kwang Moo Yi, and Andrea Tagliasacchi. Radiant foam: Real-time differentiable ray tracing. In *Proceedings of the Computer Vision and Pattern Recognition Conference*, 2025. 1, 2, 3

[17] Chun Gu, Xiaofei Wei, Zixuan Zeng, Yuxuan Yao, and Li Zhang. Irgs: Inter-reflective gaussian splatting with 2d gaussian ray tracing. In *CVPR*, 2025. 1, 2, 3, 4

[18] Alex Hanson, Allen Tu, Geng Lin, Vasu Singla, Matthias Zwicker, and Tom Goldstein. Speedy-splat: Fast 3d gaussian splatting with sparse pixels and sparse primitives. In *Proceedings of the Computer Vision and Pattern Recognition Conference (CVPR)*, pages 21537–21546, 2025. 2, 3, 4, 5, 6, 8

[19] Alex Hanson, Allen Tu, Vasu Singla, Mayuka Jayawardhana, Matthias Zwicker, and Tom Goldstein. Pup 3d-gs: Principled uncertainty pruning for 3d gaussian splatting. In *Proceedings of the Computer Vision and Pattern Recognition Conference (CVPR)*, pages 5949–5958, 2025. 2, 3, 5, 6

[20] Peter Hedman, Julien Philip, True Price, Jan-Michael Frahm, George Drettakis, and Gabriel Brostow. Deep blending for free-viewpoint image-based rendering. *ACM Trans. Graph.*, 37(6), 2018. 2, 5, 7

[21] Peter Hedman, Pratul P Srinivasan, Ben Mildenhall, Jonathan T Barron, and Paul Debevec. Baking neural radiance fields for real-time view synthesis. In *Proceedings of the IEEE/CVF international conference on computer vision*, pages 5875–5884, 2021. 2

[22] Sunghwan Hong, Jaewoo Jung, Heeseong Shin, Jiaolong Yang, Seungryong Kim, and Chong Luo. Unifying correspondence pose and nerf for generalized pose-free novel view synthesis. In *Proceedings of the IEEE/CVF Conference on Computer Vision and Pattern Recognition*, pages 20196–20206, 2024. 2

[23] Binbin Huang, Zehao Yu, Anpei Chen, Andreas Geiger, and Shenghua Gao. 2d gaussian splatting for geometrically accurate radiance fields. In *ACM SIGGRAPH 2024 Conference Papers*, New York, NY, USA, 2024. Association for Computing Machinery. 2, 4

[24] Binbin Huang, Zehao Yu, Anpei Chen, Andreas Geiger, and Shenghua Gao. 2d gaussian splatting for geometrically ac-

curate radiance fields. In *ACM SIGGRAPH 2024 conference papers*, pages 1–11, 2024. 1

[25] Shi-Sheng Huang, Guo Chen, Chen Li Heng, and Hua Huang. Neuralindicator: Implicit surface reconstruction from neural indicator priors. In *Forty-first International Conference on Machine Learning*, 2024. 2

[26] Shi-Sheng Huang, Zixin Zou, Yichi Zhang, Yan-Pei Cao, and Ying Shan. Sc-neus: Consistent neural surface reconstruction from sparse and noisy views. In *Proceedings of the AAAI conference on artificial intelligence*, pages 2357–2365, 2024. 2

[27] Zixiong Huang, Qi Chen, Libo Sun, Yifan Yang, Naizhou Wang, Qi Wu, and Mingkui Tan. G-nerf: Geometry-enhanced novel view synthesis from single-view images. In *Proceedings of the IEEE/CVF Conference on Computer Vision and Pattern Recognition*, pages 10117–10126, 2024. 2

[28] Yingwenqi Jiang, Jiadong Tu, Yuan Liu, Xifeng Gao, Xiaoxiao Long, Wenping Wang, and Yuexin Ma. Gaussianshader: 3d gaussian splatting with shading functions for reflective surfaces, 2023. 1, 3

[29] Bernhard Kerbl, Georgios Kopanas, Thomas Leimkühler, and George Drettakis. 3d gaussian splatting for real-time radiance field rendering. *ACM Transactions on Graphics*, 42(4), 2023. 1, 2, 4, 5, 6

[30] Ye Keyang, Hou Qiming, and Zhou Kun. 3d gaussian splatting with deferred reflection. *ACM SIGGRAPH Conference Proceedings, Denver, CO, United States, July 28 - August 1, 2024*, 2024. 1, 3

[31] Diederik P. Kingma and Jimmy Ba. Adam: A method for stochastic optimization, 2017. 5

[32] Arno Knapitsch, Jaesik Park, Qian-Yi Zhou, and Vladlen Koltun. Tanks and temples: benchmarking large-scale scene reconstruction. *ACM Trans. Graph.*, 36(4), 2017. 2, 5, 7

[33] Joo Chan Lee, Daniel Rho, Xiangyu Sun, Jong Hwan Ko, and Eunbyung Park. Compact 3d gaussian representation for radiance field. In *Proceedings of the IEEE/CVF Conference on Computer Vision and Pattern Recognition*, pages 21719–21728, 2024. 2, 3

[34] Deqi Li, Shi-Sheng Huang, and Hua Huang. Mpgs: Multi-plane gaussian splatting for compact scenes rendering. *IEEE Transactions on Visualization and Computer Graphics*, 2025. 1, 3

[35] Jingzhi Li, Zongwei Wu, Eduard Zamfir, and Radu Timofte. Recap: Better gaussian relighting with cross-environment captures. In *Proceedings of the Computer Vision and Pattern Recognition Conference*, pages 21307–21316, 2025. 1, 3

[36] Zhihao Liang, Qi Zhang, Ying Feng, Ying Shan, and Kui Jia. Gs-ir: 3d gaussian splatting for inverse rendering. In *Proceedings of the IEEE/CVF Conference on Computer Vision and Pattern Recognition*, pages 21644–21653, 2024. 1, 3

[37] Chin-Yang Lin, Chung-Ho Wu, Chang-Han Yeh, Shih-Han Yen, Cheng Sun, and Yu-Lun Liu. Frugalnerf: Fast convergence for extreme few-shot novel view synthesis without learned priors. In *Proceedings of the Computer Vision and Pattern Recognition Conference*, pages 11227–11238, 2025. 2

[38] Weikai Lin, Yu Feng, and Yuhao Zhu. Metasapiens: Real-time neural rendering with efficiency-aware pruning and accelerated foveated rendering. In *Proceedings of the 30th ACM International Conference on Architectural Support for Programming Languages and Operating Systems, Volume 1*, page 669–682, New York, NY, USA, 2025. Association for Computing Machinery. 2, 3, 5, 6

[39] Tao Lu, Mulin Yu, Linning Xu, Yuanbo Xiangli, Limin Wang, Dahua Lin, and Bo Dai. Scaffold-gs: Structured 3d gaussians for view-adaptive rendering. In *Proceedings of the IEEE/CVF Conference on Computer Vision and Pattern Recognition*, pages 20654–20664, 2024. 1, 3

[40] Saswat Subhajyoti Mallick, Rahul Goel, Bernhard Kerbl, Markus Steinberger, Francisco Vicente Carrasco, and Fernando De La Torre. Taming 3dgs: High-quality radiance fields with limited resources. In *SIGGRAPH Asia 2024 Conference Papers*, New York, NY, USA, 2024. Association for Computing Machinery. 3

[41] Ben Mildenhall, Pratul P. Srinivasan, Matthew Tancik, Jonathan T. Barron, Ravi Ramamoorthi, and Ren Ng. Nerf: Representing scenes as neural radiance fields for view synthesis. In *ECCV*, 2020. 2

[42] Nicolas Moenne-Loccoz, Ashkan Mirzaei, Or Perel, Ricardo de Lutio, Janick Martinez Esturo, Gavriel State, Sanja Fidler, Nicholas Sharp, and Zan Gojcic. 3d gaussian ray tracing: Fast tracing of particle scenes. *ACM Transactions on Graphics (TOG)*, 43(6):1–19, 2024. 1, 2, 3, 4

[43] Thomas Müller, Alex Evans, Christoph Schied, and Alexander Keller. Instant neural graphics primitives with a multiresolution hash encoding. *ACM transactions on graphics (TOG)*, 41(4):1–15, 2022. 2

[44] Michael Niemeyer, Fabian Manhardt, Marie-Julie Rakotosaona, Michael Oechsle, Daniel Duckworth, Rama Gosula, Keisuke Tateno, John Bates, Dominik Kaeser, and Federico Tombari. Radsplat: Radiance field-informed gaussian splatting for robust real-time rendering with 900+ fps. In *International Conference on 3D Vision 2025*, 2025. 3

[45] Steven G. Parker, James Bigler, Andreas Dietrich, Heiko Friedrich, Jared Hoberock, David Luebke, David McAllister, Morgan McGuire, Keith Morley, Austin Robison, and Martin Stich. Optix: a general purpose ray tracing engine. 29(4), 2010. 1

[46] Adam Paszke, Sam Gross, Francisco Massa, Adam Lerer, James Bradbury, Gregory Chanan, Trevor Killeen, Zeming Lin, Natalia Gimelshein, Luca Antiga, Alban Desmaison, Andreas Köpf, Edward Yang, Zach DeVito, Martin Raison, Alykhan Tejani, Sasank Chilamkurthy, Benoit Steiner, Lu Fang, Junjie Bai, and Soumith Chintala. *PyTorch: an imperative style, high-performance deep learning library*. Curran Associates Inc., Red Hook, NY, USA, 2019. 5

[47] Christian Reiser, Songyou Peng, Yiyi Liao, and Andreas Geiger. Kilonerf: Speeding up neural radiance fields with thousands of tiny mlps. In *Proceedings of the IEEE/CVF international conference on computer vision*, pages 14335–14345, 2021. 2

[48] Kerui Ren, Lihan Jiang, Tao Lu, Mulin Yu, Linning Xu, Zhangkai Ni, and Bo Dai. Octree-gs: Towards consistent

real-time rendering with lod-structured 3d gaussians. *IEEE Transactions on Pattern Analysis and Machine Intelligence*, 2025. 1, 3

[49] Rafał Tobiasz, Grzegorz Wilczyński, Marcin Mazur, Sławomir Tadeja, and Przemysław Spurek. Meshsplat: Mesh-based rendering with gaussian splatting initialization. *arXiv preprint arXiv:2502.07754*, 2025. 1

[50] Dor Verbin, Peter Hedman, Ben Mildenhall, Todd Zickler, Jonathan T. Barron, and Pratul P. Srinivasan. Ref-nerf: Structured view-dependent appearance for neural radiance fields. In *2022 IEEE/CVF Conference on Computer Vision and Pattern Recognition (CVPR)*, pages 5481–5490, 2022. 2, 5, 6, 7, 8

[51] Dor Verbin, Pratul P. Srinivasan, Peter Hedman, Ben Mildenhall, Benjamin Attal, Richard Szeliski, and Jonathan T. Barron. Nerf-casting: Improved view-dependent appearance with consistent reflections. In *SIGGRAPH Asia 2024 Conference Papers*, New York, NY, USA, 2024. Association for Computing Machinery. 2, 5, 6, 7, 8

[52] Peng Wang, Lingjie Liu, Yuan Liu, Christian Theobalt, Taku Komura, and Wenping Wang. Neus: Learning neural implicit surfaces by volume rendering for multi-view reconstruction. *arXiv preprint arXiv:2106.10689*, 2021. 2

[53] Zhou Wang, A.C. Bovik, H.R. Sheikh, and E.P. Simoncelli. Image quality assessment: from error visibility to structural similarity. *IEEE Transactions on Image Processing*, 13(4):600–612, 2004. 5

[54] Qi Wu, Janick Martinez Esturo, Ashkan Mirzaei, Nicolas Moenne-Loccoz, and Zan Gojcic. 3dgut: Enabling distorted cameras and secondary rays in gaussian splatting. In *Proceedings of the Computer Vision and Pattern Recognition Conference*, pages 26036–26046, 2025. 1, 2, 3, 4

[55] Tao Xie, Xi Chen, Zhen Xu, Yiman Xie, Yudong Jin, Yujun Shen, Sida Peng, Hujun Bao, and Xiaowei Zhou. Envgs: Modeling view-dependent appearance with environment gaussian. In *2025 IEEE/CVF Conference on Computer Vision and Pattern Recognition (CVPR)*, pages 5742–5751, 2025. 1, 2, 3, 4, 5, 6, 7, 8

[56] Jingwei Xu, Yikai Wang, Yiqun Zhao, Yanwei Fu, and Shenghua Gao. 3d streetunveiler with semantic-aware 2dgs - a simple baseline. In *The International Conference on Learning Representations (ICLR)*, 2025. 1, 3

[57] Zhen Xu, Tao Xie, Sida Peng, Haotong Lin, Qing Shuai, Zhiyuan Yu, Guangzhao He, Jiaming Sun, Hujun Bao, and Xiaowei Zhou. Easyvolcap: Accelerating neural volumetric video research. In *SIGGRAPH Asia 2023 Technical Communications*, New York, NY, USA, 2023. Association for Computing Machinery. 5

[58] Yuxuan Yao, Zixuan Zeng, Chun Gu, Xiatian Zhu, and Li Zhang. Reflective gaussian splatting. In *ICLR*, 2025. 1, 2, 3, 5, 6

[59] Yuxuan Yao, Zixuan Zeng, Chun Gu, Xiatian Zhu, and Li Zhang. Reflective gaussian splatting. In *ICLR*, 2025. 6

[60] Richard Zhang, Phillip Isola, Alexei A. Efros, Eli Shechtman, and Oliver Wang. The unreasonable effectiveness of deep features as a perceptual metric. In *2018 IEEE/CVF Conference on Computer Vision and Pattern Recognition*, pages 586–595, 2018. 5

[61] Wenyuan Zhang, Jimin Tang, Weiqi Zhang, Yi Fang, Yu-Shen Liu, and Zhizhong Han. Materialrefgs: Reflective gaussian splatting with multi-view consistent material inference. In *NeurIPS*, 2025. 3

[62] Zuo-Liang Zhu, Jian Yang, and Beibei Wang. Gaussian splatting with discretized sdf for relightable assets. In *Proceedings of the IEEE/CVF International Conference on Computer Vision*, pages 25155–25164, 2025. 1, 3

[63] Zi-Xin Zou, Shi-Sheng Huang, Yan-Pei Cao, Tai-Jiang Mu, Ying Shan, Hongbo Fu, and Song-Hai Zhang. Gp-recon: Online monocular neural 3d reconstruction with geometric prior. *IEEE Transactions on Visualization and Computer Graphics*, 2024. 2